Boiling & Condensation 2015

9th International Conference on Boiling and Condensation Heat Transfer
April 26-30, 2015 – Boulder, Colorado

DESIGN SENSITIVITY ANALYSIS OF USING VARIOUS FLOW BOILING CORRELATIONS FOR A DIRECT EVAPORATOR IN HIGH-TEMPERATURE WASTE HEAT RECOVERY ORCS

Alihan Kaya*, Steven Lecompte, Marija Lazova, Kathleen De Kerpel and Michel De Paepe
*Author for correspondence
Department of Flow, Heat and Combustion Mechanics
Ghent University
Ghent, 9000, Belgium
E-mail: alihan.kaya@ugent.be

ABSTRACT

High-temperature waste heat (250°C-400°C) sources being created by industrial operations such as metallurgical industry, incinerators, combustion engines, annealing furnaces, drying, baking, cement production etc. are being utilized in Organic Rankine cycle (ORC) waste heat recovery systems. Alongside indirect ORC evaporators having intermediate heat carrier loops, ORC waste heat recovery can also be done through a direct evaporator (e.g. tube bundles) applied on a heat source. In an evaporator design problem, the accuracy of the design method has a significant impact on the end result. In that manner, for revealing the design accuracy error margin of using various flow boiling heat transfer methods, a design sensitivity analysis is performed by means of using 13 different flow boiling heat transfer correlations. All correlations are implemented separately into an iterative evaporator calculation and the resulting sizing solutions are compared for a representative high-temperature waste heat recovery evaporator case. The volumetric flow rate of the waste heat is 80000 Nm³/h and the inlet temperature is 375°C. The considered working fluid is cyclopentane and the deduced optimal evaporation temperature (OET) is 227°C. The minimum corresponding total transferred heat in the evaporator is at least 3,5 MW in all calculations.

INTRODUCTION

In the last decades, waste heat recovery through Organic Rankine cycles (ORCs) has been studied by many researchers. This tendency is in parallel with the increasing concerns over shortage of energy, ozone depletion and global warming, being caused by old refrigerants which are reported to be harmful for the environment and currently being phased out. ORCs have a similar working principal with the conventional Rankine cycle, but they utilize a low Global Warming Potential (GWP) and Ozone Depletion Potential (ODP) organic fluid as working fluid in the thermodynamic cycle, instead of water or steam. ORCs have a wide range of applications where a waste heat source is being created by industrial operations such as metallurgical industry, incinerators, combustion engines, annealing furnaces, drying, baking, cement production etc. ORCs are typically being applied on waste heat sources with the temperature range from 100°C up to 400°C, by being usually referred as low-temperature waste heat (100°C-250°C) and high-temperature waste heat (250°C-400°C).

Table 1: Promising working fluids for high-temperature ORCs

Working Fluid	T_c (K)	P_c (MPa)	T_{AI} (K)
n-Butane	425,20	3,922	638,15
n-Pentane	469,65	3,370	582,15
Cyclopentane	511,70	4,510	634,15
MM	518,70	1,925	613,15
MDM	564,13	1,415	623,15
Toluene	591,80	4,109	753,15

The case-specific working conditions are the main determining parameters for the cycle design. The efficiency of the cycle strongly depends on the considered working fluid. A reasonable selection process can be done by taking the fluids' thermodynamic, stability, safety, legislative and environmental aspects into consideration for a particular case. The critical temperature and critical pressure values of the working fluid are the main criterion for distinguishing the cycle conditions (subcritical, transcritical and supercritical) of an ORC. Some of the promising working fluids for high-temperature waste heat recovery ORCs are listed in Table 1. The listed fluids have very low GWP and zero ODP, as well as critical temperatures higher than 150°C and auto ignition temperatures in the safe zone for present case (>300°C). Cyclopentane is selected for the case, in the light of its reported advantages in high-temperature ORCs (Pierobon et al., 2013, Lai et al., 2011, Shu et al., 2014).

Alongside indirect ORC evaporators having intermediate heat carrier loops, ORC waste heat recovery can also be done through a direct evaporator (e.g. tube bundles) applied on a heat source (Ribatski and Thome, 2007). The thermodynamic efficiency of an evaporator relies on heat transfer and pressure drops, and thus, the sizing of an evaporator is performed accordingly (Quoilin et al, 2013). In a design problem, the accuracy of the design method has a significant impact on the end result. A too small sized evaporator will not be capable of evaporating the refrigerant completely at the evaporator outlet, which might cause turbine or expander damage in some cases. On the other hand, a rather large evaporator yields working fluid superheating, which may lead to a negative impact on system performance and a higher heat exchanger cost (Fischer, 2011).

Even though the design of evaporator for waste heat recovery ORC applications is significantly dependent on flue gas flow conditions outside the tube (waste heat carrier side), the accuracy of in-tube flow boiling calculations might have a visible influence on the sizing problem. For revealing the error margin of using various flow boiling heat transfer methods, a design sensitivity analysis is performed by means of using 13 different flow boiling heat transfer correlations, where Kandlikar's correlation (Kandlikar, 1990) is taken as the reference. The correlations are listed in Table 2.

Table 2: Used flow boiling correlations

Author(s)	Year	Source
Kandlikar	1990	(Kandlikar, 1990)
Chun & Seban	1971	(Krupiczka et al., 2002)
Gungor & Winterton	1986	(Gungor & Winterton, 1986)
Wattelet et al.	1994	(Zhou et al., 2013)
Butterworth	1970	(Collier & Thome, 1994)
Chen	1966	(Thome, 2004)
Bennett et al.	1959	(Kandlikar, 1990)
Palen	1983	(Thome, 2004)
Shah	2009	(Shah, 2009)
Klimenko	1990	(Bao et al., 2000)
Liu & Winterton	1991	(Ghiaasiaan, 2007)
Kattan-Thome-Favrat	1998	(Thome, 2004)
Steiner & Taborek	1992	(Ghiaasiaan, 2007)

All correlations are implemented separately into an iterative evaporator calculation and the resulting sizing solutions are compared for a representative high-temperature waste heat recovery evaporator case. For the outer-side heat transfer calculations, VDI-Wärmeatlas method (VDI-Heat Atlas, 2010) was used. The convective coefficients for the superheated single-phase zones occurring close to the outlet of serpentine tubes are calculated through Dittus-Boelter equation. For evaluating the in-tube and outer pressure drops, Friedel correlation (Friedel, 1979) and Robinson&Briggs correlation (Thome, 2004) is used, respectively. For calculating the two-phase pressure drop at U-bends, Muller-Steinhagen-Heck correlation (Müller-Steinhagen and Heck, 1986) is used. The volumetric flow rate of the waste heat is 80000 Nm^3/h and the inlet temperature is 375°C. The considered working fluid is cyclopentane. The case specific optimal evaporation temperature (OET) is 227°C, and calculated through the method of Lecompte et al. (Lecompte et al, 2013). The minimum corresponding total transferred heat in the evaporator is at least 3,5 MW in all calculations. The fouling outside (industrial flue gas) and inside the tubes (working fluid) are determined as 0,0004 m^2K/W and 0,0002 m^2K/W, respectively. Saturated liquid ($x=0$) coming from an economizer (not included in the model) is assumed to enter at the inlet of the evaporator. Considered heat exchanger specifications can be seen in the Table 3.

Table 3: Assumed specifications of the direct evaporator

Tube Outer Diameter (mm)	38
Tube Wall Thickness(mm)	2,77
One Tube Length (m)	4
Heat Exchanger Width (m)	3
Tube Material	Carbon Steel
Fin Diameter (mm)	70
Fin Thickness (mm)	0,4
Fin Density (fin/m)	432
Fin Material	Aluminum
U-Bend Diameter (mm)	114(3xTube Dia)
Tube Layout	Staggered
Transverse Pitch (mm)	73
Longitudinal Pitch (mm)	108

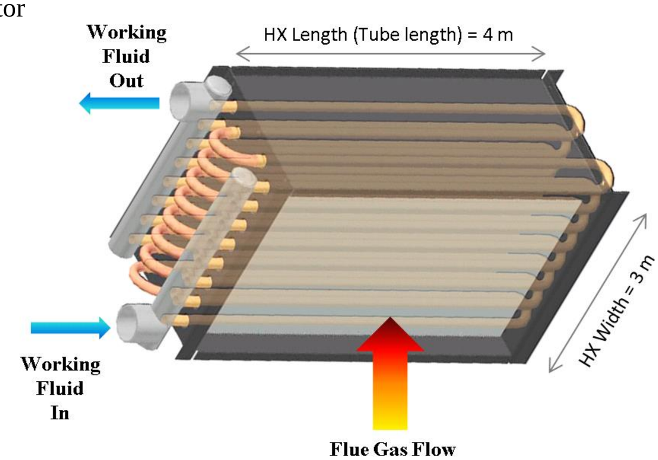

Figure 1: Representative illustration of the direct evaporator

The fan power is calculated as:

$$Fan\ Power = G_h A_{min} \frac{\Delta P_{air}}{\rho_h{}^{0.85}} \quad (1)$$

where the fan efficiency of 85% is assumed. The cost estimation is for comparative reasons and is made by considering updated European market values of carbon steel tubing and U-bend welding labor cost, whereas the fin cost is excluded.

DESIGN SENSITIVITY ANALYSIS

The deviation (absolute value) in each of said parameters depending on the correlations are illustrated in Figures 1-6, whereas their h_{tp} deviations are also illustrated for the sake of clarifying the flexibility of correlation usage for the present case. In the following graphs, left ones of pillar pairs represent the deviations of h_{tp} values of each correlation in comparison to Kandlikar's correlation. On the other hand, the right ones of pillar pairs show how much does h_{tp} deviations influence the investigated design parameters. The zero value of any pillar means that the correlation yields the same design result and the corresponding h_{tp} deviation is lower than design resolution, thus, can be used instead of Kandlikar's correlation for the specified condition. It is important to note that the deviations of cost, total tube length, count of number of U-bends and longitudinal heat exchanger length are quite similar as they are directly related to each other. Figures 2-4 show thermo-economic parameters such as manufacturing cost, fan power and total transferred heat.

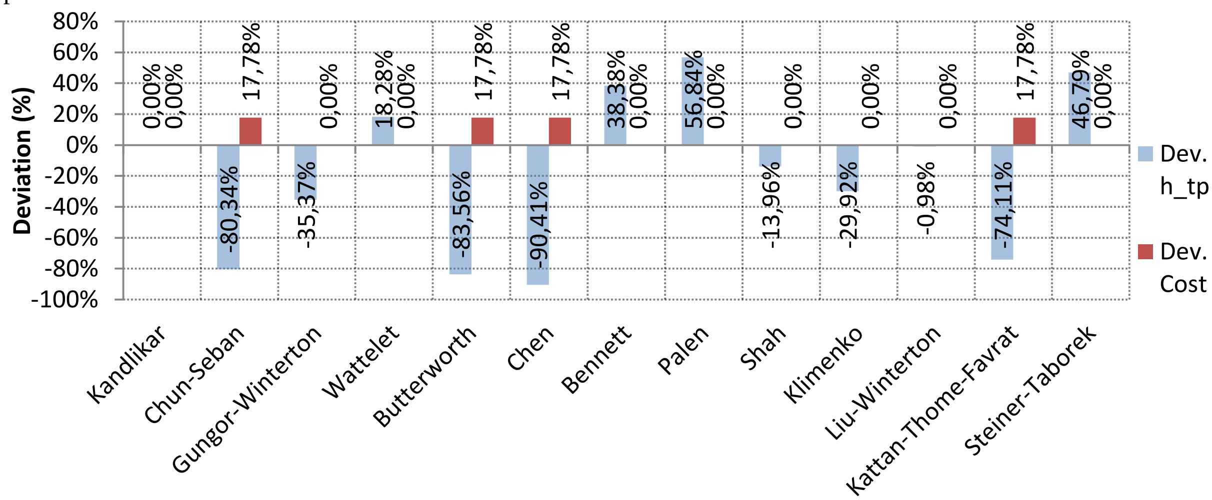

Figure 2: Influence of deviation in h_{tp} on estimated manufacturing cost (@D_{out}=1- ½", t_w=2,77 mm and P_f=432 fin/m)

Chun-Seban, Butterworth, Chen and Kattan-Thome-Favrat correlations underpredict the heat transfer coefficients which yields to a higher cost estimation by 17,78%. All other correlations appear to be interchangeable. It seems so that overpredicting the heat transfer coefficients up to 56,84% (i.e. Palen) and down to 35,37% underprediction (i.e. Gungor & Winterton) do not have any observable effect on cost estimation. The step change of cost is due to the step change in calculated tube length. Figure 3 shows the deviation on estimated required industrial fan power.

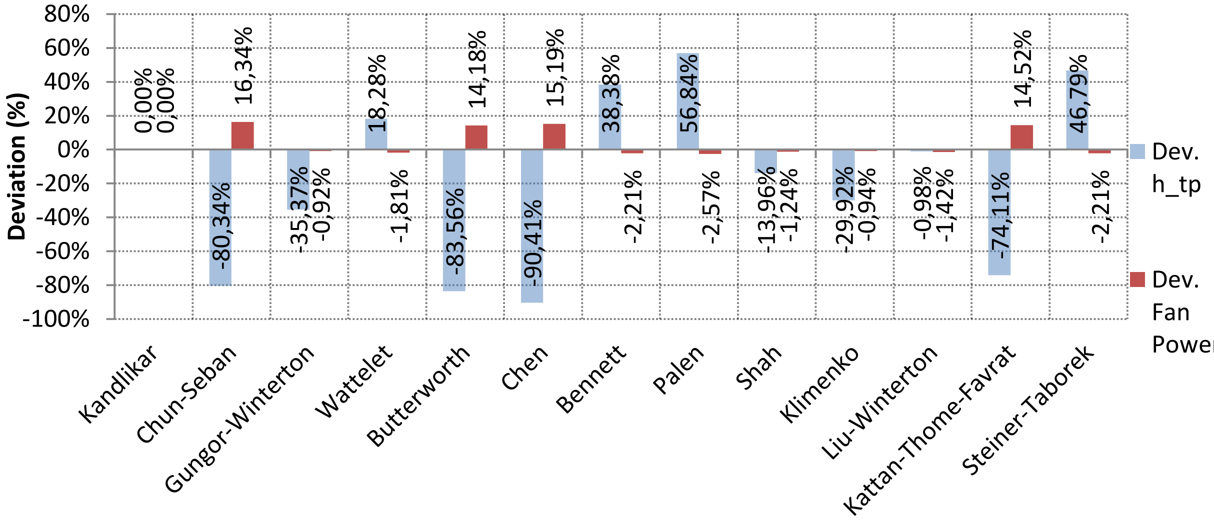

Figure 3: Influence of deviation in h_{tp} on estimated fan power (@D_{out}=1- ½”, t_w=2,77 mm and P_f=432 fin/m)

Similar to the previous results, the underprediction of Chun-Seban, Butterworth, Chen and Kattan-Thome-Favrat correlations yields up to 16,34% higher required fan power. In accordance to those, total deviation of fan power estimation does not exceed 18,91%. When the underpredicting group is ignored, the deviation between other correlations does not exceed 2,57%, which is caused by the 56,84% overprediction of Palen correlation. Figure 4 shows the deviations of calculated total transferred heat from flue gas to the finned-tube bundle of the direct evaporator.

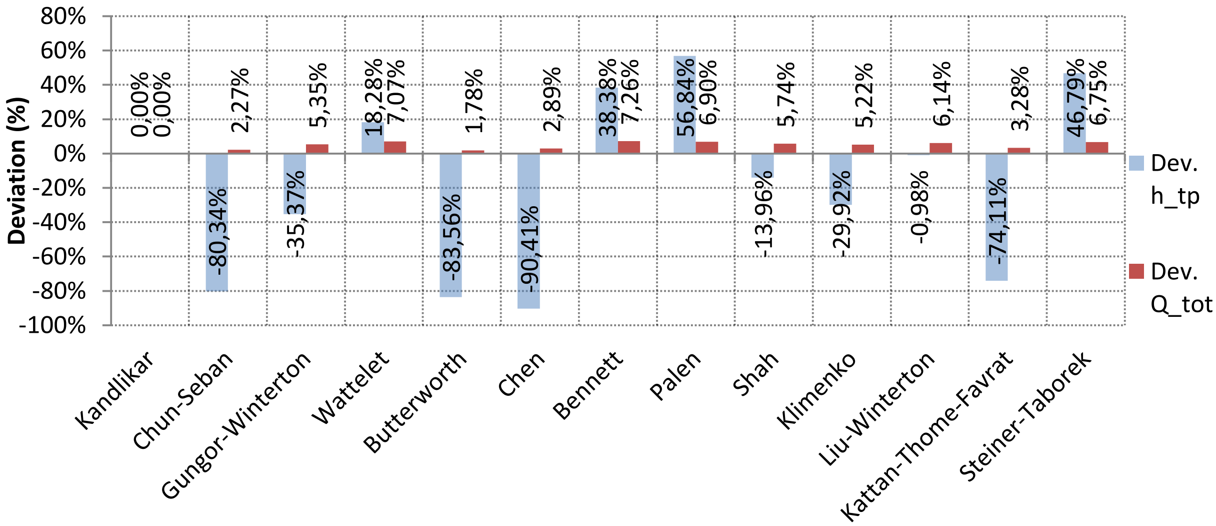

Figure 4: Influence of deviation in h_{tp} on calculated total transferred heat (@D_{out}=1- ½”, t_w=2,77 mm and P_f=432 fin/m)

The transferred heat estimation deviation does not exceed 7,26% overall. The heat transfer coefficient underprediction of Chun-Seban, Butterworth, Chen and Kattan-Thome-Favrat correlations does not lead to any significant deviation in total transferred heat. Bennett correlation predicts the highest Q_{tot}. Kandlikar’s correlation predicts the lowest transferred heat. From the aspect of total transferred heat, correlations seem to be interchangeable, even under convective coefficient deviations up to 90,41%. Figures 5-7 show the deviations of air-side overall heat transfer coefficient U_h, air-side pressure drop ΔP_{air} and refrigerant side two-phase pressure drop ΔP_{ref} are compared with the changing h_{tp}.

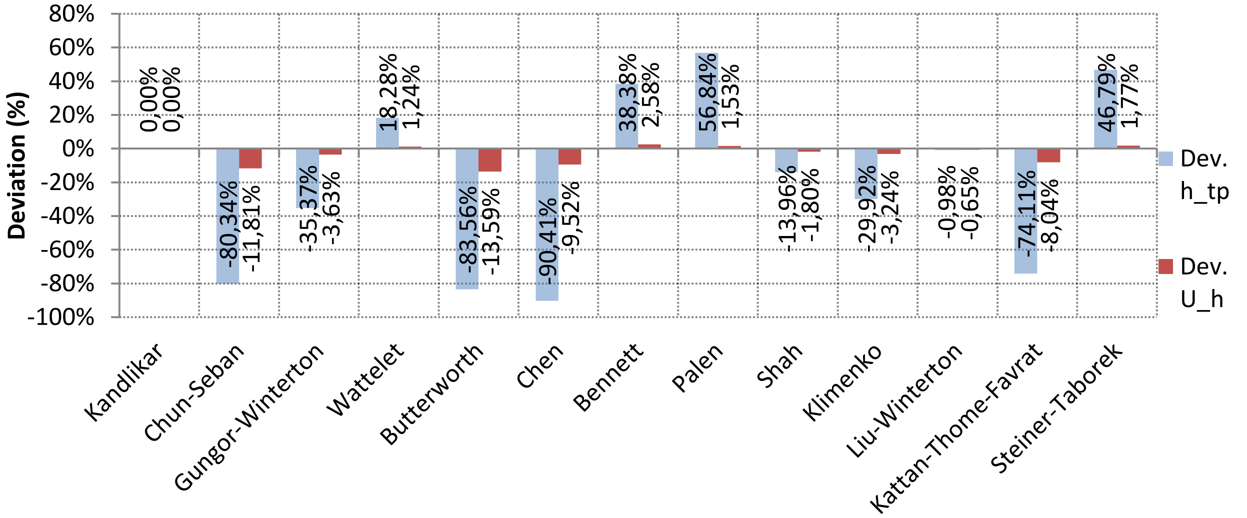

Figure 5: Influence of deviation in h_{tp} on overall air-side heat transfer coefficient (@D_{out}=1- ½", t_w=2,77 mm and P_f=432 fin/m)

Due the fact that the design is mainly air-side convection dependent, the deviations do not differ crucially. The highest deviation of overall air-side heat transfer coefficient (16,17%) occurred between Bennett and Butterworth correlations. Similar to the previous prediction behaviors, Chun-Seban, Chen and Kattan-Thome-Favrat correlations show relatively large deviations as well. The rest of the methods do not deviate more than 3,63% in comparison to Kandlikar's correlation and 5,16% among each other. Figure 6 shows the deviations of air-side pressure drop.

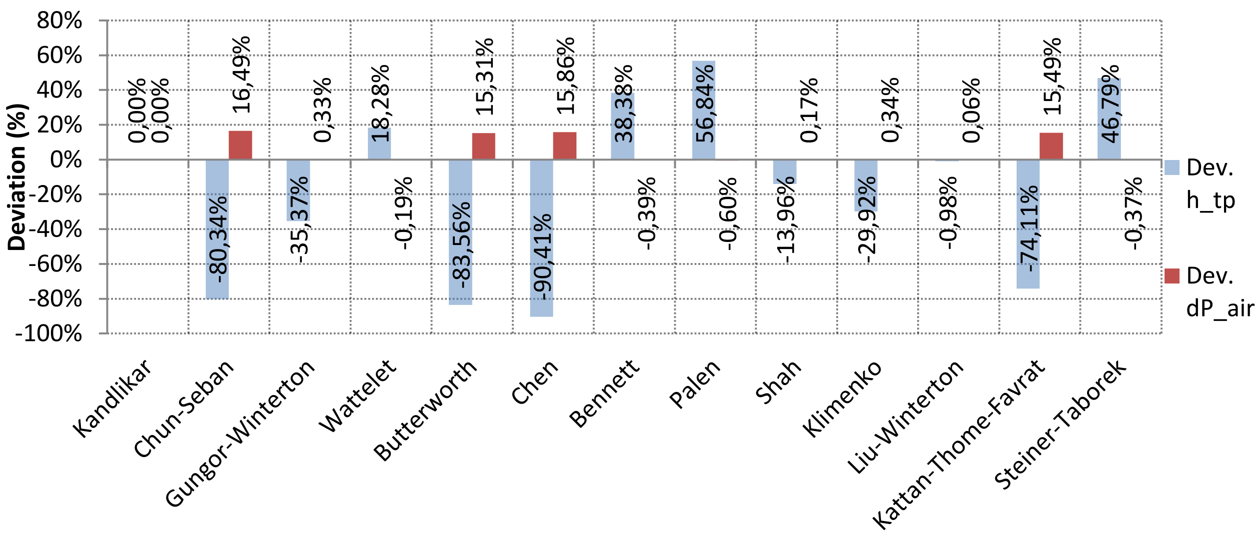

Figure 6: Influence of deviation in h_{tp} on air-side pressure drop (@D_{out}=1- ½", t_w=2,77 mm and P_f=432 fin/m)

The air-side pressure drops show a maximum deviation of 17,47% among each other. The big difference of Chun-Seban, Butterworth, Chen and Kattan-Thome-Favrat correlations in comparison to the rest due to the higher number of rows through which the air propagates longitudinally. When the underpredicting correlations are neglected, largest deviation is calculated as 1,32%. Figure 7 shows the deviations of in-tube two phase pressure drop.

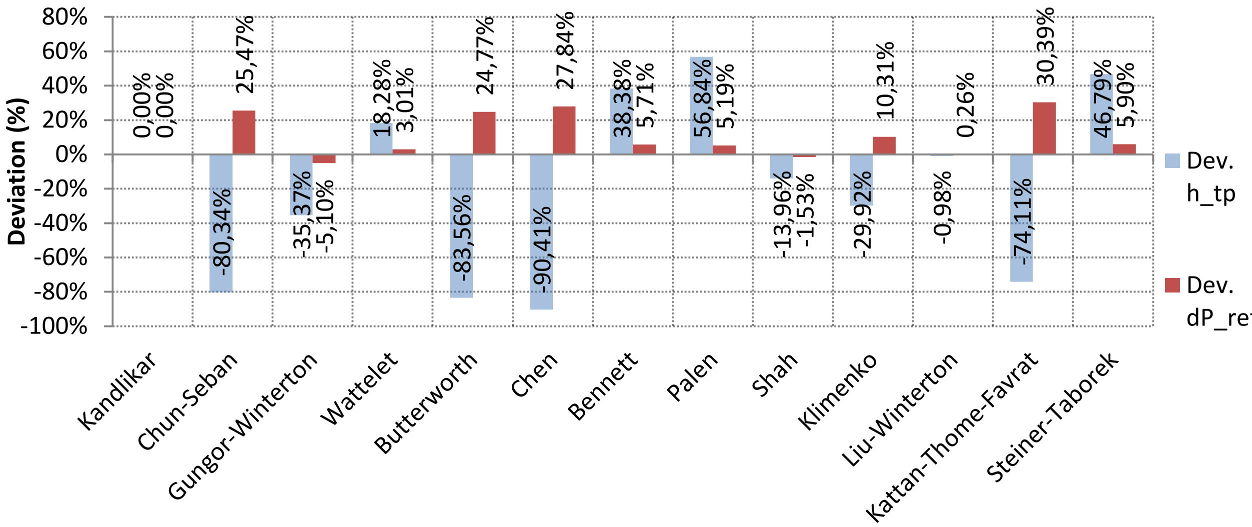

Figure 7: Influence of deviation in h_{tp} on in-tube pressure drop (@D_{out}=1- ½”, t_w=2,77 mm and P_f=432 fin/m)

Due to the fact that in-tube two phase pressure drop is strongly related to the serpentine tube length along where the working fluid propagates, Chun-Seban, Chen and Kattan-Thome-Favrat correlations deviate comparatively more (up to 35,49%). The rest demonstrate relatively minor deviations, up to 15,41% among each other.

CONCLUSIONS

A design sensitivity analysis of 13 correlations for a direct ORC evaporator for high-temperature waste heat recovery applications is performed. By that means, a deeper insight about the error margin in designing direct ORC evaporators for high-temperature waste heat recovery applications is obtained. According to the results following conclusions are made:

- Older methods such as Chun & Seban, Butterworth and Chen correlations lead to larger error margin in design, up to 35,49%,
- Kattan-Thome-Favrat has an underpredicting estimation in comparison to the Kandlikar correlation,
- Kandlikar, Gungor & Winterton, Wattelet, Bennett, Palen, Shah, Klimenko, Liu & Winterton and Steinter & Taborek methods may be used interchangeably,
- When more updated prediction methods are interchangeably used, error margins remain lower than 15,41% for the in-tube two phase pressure drop estimation and less than 7,26% in the rest of investigated parameters,
- The correlations may be used interchangeably for design reasons, especially when their own accuracies are taken into consideration,
- Experimental research is necessary to reveal the prediction capacity of considered correlations.

NOMENCLATURE

A_{min}	Minimum flow area between tube bundle, m²
D_{out}	Tube outer diameter, m
G_h	Air mass flux, kg/m²s
h_{tp}	Two-phase heat transfer coefficient, W/m²K
L	Total tube length, m
L_{hx}	Longitudinal heat exchanger length, m
P_f	Fin pitch, fins/m
t_w	Wall thickness, m
Q_{tot}	Total transferred heat, W
ΔP_{air}	Air-side pressure drop, Pa
ΔP_{ref}	Refrigerant-side pressure drop, Pa
ρ_h	Air density, units

REFERENCES

Pierobon L., Nguyen T.V., Larsen U., Haglind F., Elmegaard B., 2013. Multi-objective optimization of organic Rankine cycles for waste heat recovery: Application in an offshore platform. Energy, 58, 538-549.

Lai N.A., Wendland M., and Fischer J., 2011. Working fluids for high-temperature organic Rankine cycles. Energy, *36*(1), 199-211.

Shu G., Li X., Tian H., Liang X., Wei H., Wang, X., 2014. Alkanes as working fluids for high-temperature exhaust heat recovery of diesel engine using organic Rankine cycle. Applied Energy, 119, 204-217.

Ribatski G., Thome J.R., 2007. Two-Phase Flow and Heat Transfer across Horizontal Tube Bundles-A Review, Heat transfer engineering 28(6), 508-524.

Quoilin S., van den Broek M., Declaye S., Dewallef P., and Lemort V., 2013. Techno-economic survey of Organic Rankine Cycle (ORC) systems. Renewable and Sustainable Energy Reviews 22, 168-186.

Fischer J., 2011. Comparison of trilateral cycles and organic Rankine cycles. Energy 36, 6208-6219.

Kandlikar S.G., 1990. A General Correlation for Saturated Two-Phase Flow Boiling Heat Transfer Inside Horizontal and Vertical Tubes. J. Heat Transfer 112, 219-228.

Krupiczka, R., Rotkegel, A., Ziobrowski, Z., 2002. Heat transfer to evaporating liquid films within a vertical tube. Chemical Engineering and Processing: Process Intensification, 41(1), 23-28.

Gungor, K. E., Winterton, R. H. S., 1986. A general correlation for flow boiling in tubes and annuli. International Journal of Heat and Mass Transfer, 29(3), 351-358.

Zhou, Z., Fang, X., Li, D., 2013. Evaluation of correlations of flow boiling heat transfer of R22 in horizontal channels. The Scientific World Journal, 2013, 14 pages.

Collier, J. G., Thome, J. R., 1994. *Convective boiling and condensation*. Oxford university press.

Thome, J. R., 2004. Engineering data book III. Wolverine Tube Inc.

Shah, M. M., 2009. An improved and extended general correlation for heat transfer during condensation in plain tubes. HVAC&R Research, 15(5), 889-913.

Bao, Z. Y., Fletcher, D. F., Haynes, B. S., 2000. Flow boiling heat transfer of Freon R11 and HCFC123 in narrow passages. International Journal of Heat and Mass Transfer, 43(18), 3347-3358.

Ghiaasiaan, S. M., 2007. Two-phase flow, boiling, and condensation: in conventional and miniature systems. Cambridge University Press.

VDI-Gesellschaft Verfahrenstechnik und Chemieingenieurwesen, & VDI Gesellschaft (Eds.). 2010. *VDI Heat Atlas*. Springer.

Friedel, L., 1979. Improved friction pressure drop correlations for horizontal and vertical two-phase pipe flow. European two-phase flow group meeting, Paper E 2, 1979.

Thome, J. R., 2004. Engineering data book III. Wolverine Tube Inc.

Müller-Steinhagen, H., Heck, K., 1986. A simple friction pressure drop correlation for two-phase flow in pipes. Chemical Engineering and Processing: Process Intensification 20(6), 297-308.

Lecompte, S., Huisseune, H., van den Broek, M., De Schampheleire, S., & De Paepe, M. (2013). Part load based thermo-economic optimization of the Organic Rankine Cycle (ORC) applied to a combined heat and power (CHP) system. *Applied Energy*, *111*, 871-881.